sustainability

MDPI

Article

Left-Side On-Ramp Metering for Improving Safety and Efficiency in Underground Expressway Systems

Minhua Shao [1,2], Congcong Xie [1,2], Lijun Sun [1,2], Xiaomin Wan [1,2] and Zhang Chen [1,2,*]

1 School of Transportation Engineering, Tongji University, 4800 Cao'an Highway, Shanghai 201804, China; shaominhua@tongji.edu.cn (M.S.); x_cc@tongji.edu.cn (C.X.); ljsun@tongji.edu.cn (L.S.); wxm1059827633@163.com (X.W.)

2 Key Laboratory of Road and Traffic Engineering of the Ministry of Education, Tongji University, Shanghai 201804, China

* Correspondence: czy1620@263.net; Tel.: +86-1391-816-0520; Fax: +86-2169585709

Received: 1 May 2019; Accepted: 4 June 2019; Published: 12 June 2019

check for updates

Abstract: As one of the effective measures of intelligent traffic control, on-ramp metering is often used to improve the traffic efficiency of expressways. Existing on-ramp metering research mainly discusses expressways with right-side on-ramps. However, for underground expressway systems (UESs), left-side on-ramps are frequently adopted to reduce the ground space occupied by ramp construction. Since traffic entering from the left and right sides of the mainline may have different traffic characteristics, on-ramp metering for UESs with left-side on-ramps should be explored specifically. This study examines the impacts of left-side on-ramps on the traffic safety and efficiency of UESs and proposes an effective on-ramp metering strategy. Firstly, using field data, traffic flow fundamental diagrams and speed dispersion are discussed to explore the traffic flow characteristics of the "left-in" UES. The results show that the capacity and critical occupancy are both reduced in left-side on-ramp compared to right-side on-ramp expressways. Meanwhile, the speed dispersion is higher in left-side on-ramp UESs, which means a higher accident risk. Based on this, considering traffic safety and efficiency, a novel two-parameter left-side on-ramp metering strategy for UESs is proposed, in which occupancy and speed are used as the control indicators simultaneously. Additionally, the mechanism of the metering strategy is explained. Finally, the proposed on-ramp metering strategy is simulated on a real UES. The results demonstrate the advantages of the proposed two-parameter on-ramp metering strategy for improving the traffic safety and efficiency of UESs.

Keywords: intelligent transportation systems; traffic safety; urban underground expressway; traffic flow characteristics; left-side on-ramp; ramp metering

1. Introduction

Due to land availability restrictions for roads in urban areas, it has become more difficult for the surface and elevated road system to meet the growing traffic demand, which has resulted in aggravated traffic congestion and serious environmental pollution [1]. An urban underground expressway system (UES) has been constructed in many cities to save land resources, alleviate traffic congestion, and improve the urban environment [2,3]. The relatively enclosed internal space of UESs and the lack of roadside references can increase drivers' psychological pressure and lead to excessive speeding, which brings traffic safety hazards [4–7].

Ensuring the traffic safety and efficiency of UESs is critical [8–11]. As one of the effective measures of intelligent traffic control, on-ramp metering is often used to improve traffic efficiency of urban expressways [12–14]. On-ramp metering strategies such as Demand-Capacity, Occupancy-Capacity, and ALINEA (the acronym for 'Asservissement line' aire d'entre' e autoroutie') [15–17] regulate on-ramp flow into mainline to alleviate traffic congestion on mainline. Makigami and Matsuo [18] also argued that measures such as on-ramp metering can provide better traffic inflow conditions for vehicles to merge into the mainline from the on-ramp, which can improve the traffic conditions. Over the years, a number of on-ramp metering strategies have been exploited. A self-adjusted fuzzy local ramp metering strategy was proposed by Gao [19] to keep the mainline traffic state and the on-ramp queue length at reasonable levels. Majid et al. [20] proposed an integrated approach for on-ramp metering using sliding mode control to avoid mainline congestion. Based on the Model Predictive Control framework, Fang et al. [21] presented an on-ramp metering algorithm to predict and assess future traffic conditions, which aims at optimizing the network mobility. Most of the existing studies on on-ramp metering are aimed at improving the traffic efficiency and have concentrated on the typical right-side on-ramps.

For countries and regions that drive on the right-hand-side, this "left-in" or "left-out" traffic organization form (that is, the traffic flow enters or leaves the mainline from the left-side on-ramps) does not conform to driving habits, which may lead to different traffic characteristics compared to the traditional "right-in" or "right-out" form. Several studies [22,23] have explored the safety and operational effects of left-side off-ramps at expressway diverging areas in Florida. These studies all concluded that left-side off-ramps are associated with a higher crash frequency than right-side off-ramps. Chen et al. [24] collected the crash records for 11 left-side and 63 similar right-side off-ramps, and the analysis results indicated that the crash rate and annual average crash frequency were significantly higher for left-side than for right-side off-ramps.

However, despite this, to the best of our knowledge, few engineering applications with left-side on-ramps have been carried out, and the limited existing studies about the effects of the "left-in" form were based on simulation experiments. A simulated driving test was conducted by Liu [25] to study the driving behavior characteristics of vehicles entering the mainline from the left- and right-side on-ramps. The results showed that speed dispersion is higher when vehicles enter the mainline of the underground expressway from a left-side on-ramp, indicating that drivers are not familiar with entering from this way, which leads to unstable driving behavior. Fang et al. [26] studied the vehicle operation characteristics at the on-ramps of the underground expressway based on a driving simulator and found that the layout of the ramp (left- vs. right-side) had a significant influence on the operation characteristics of vehicles entering from the on-ramps. Eustace et al. [27] analyzed the effects of merging areas in the vicinity of on-ramps on crash frequency, and the results indicated that crashes are more likely to occur in merging areas near the left-side on-ramps.

These literatures indicate that there are significantly different traffic characteristics between the right- and left-side on-ramp expressways. Although these results need to be further backed up by real applications, it can still be concluded that the existing on-ramp metering methods for right-side ramps are not appropriate for left-side ramps. Traditional on-ramp metering has generally focused on traffic efficiency, but safety should also be emphasized in the left-side on-ramp metering. However, left-side ramps are frequently adopted in the UES to reduce the land space occupied by the ramps. No relevant research has been found on the on-ramp metering of underground expressways with left-side on-ramps. To sum up, left-side on-ramp metering represents a palpable research gap in the on-ramp metering model, which is also an important method in the traffic management of the UES.

To develop a left-side on-ramp metering strategy, it is necessary to improve the understanding of the "left-in" UES traffic flow characteristics as a first step. In this paper, the Shanghai Bund Underground Expressway was investigated as a real left-side on-ramp UES application. The traffic flow characteristics were analyzed using field data by first comparing them to those of a similar expressway with a right-side on-ramp. The target occupancy and speed for on-ramp metering were determined based on the traffic efficiency, safety, and efficiency of road infrastructure utilization. Then, a two-parameter on-ramp metering strategy was proposed for the left-side on-ramp UES. After applying the two-parameter metering strategy and the traditional ALINEA method to the Shanghai Bund Underground Expressway, the performance of the proposed control strategy was examined.

The main contributions of this paper are the determination of the empirical traffic flow characteristics of the "left-in" UES and the development of an efficient left-side on-ramp metering strategy for UESs.

2. Traffic Characteristics Analysis of "Left-In" UES

A typical "left-in" underground expressway and a traditional expressway with a right-side on-ramp were selected, which have similar traffic organization characteristics. The three-parameter relationship of traffic flow and the speed dispersion between the two expressways were compared and analyzed to determine the empirical traffic flow characteristics of the "left-in" UES.

2.1. Subject Selection and Data Sources

The Shanghai Bund Underground Expressway, which has left-side on-ramps, was investigated in this study. Built in 2010, it starts from Laotaiping Lane in Zhongshan South Road and ends at Haining Road. The section between the left-side on-ramp of East Changzhi Road and the right-side off-ramp of Yan'an East Road was selected as the research object. It is equipped with coil detectors. However, their time interval for data output is 1 h, which did not meet the requirements for the study. Fortunately, the Bund Underground Expressway has an integrated video monitoring system that can be used to collect traffic data; this was used as the data source for this study. The basic sketch of the research section is shown in Figure 1. Considering the position of the video camera, the approximate position of the selected detection section is as shown by the red line in the figure.

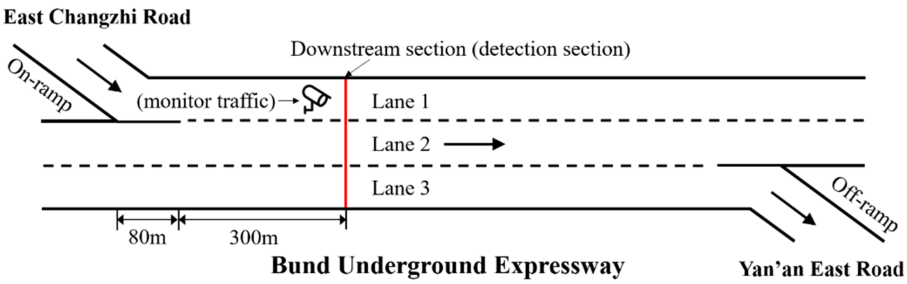

Figure 1. Sketch of "left-in" research section.

The method of collecting the detection data for the research section based on the video is shown in Figure 2, and data such as traffic flow, speed, and occupancy were acquired at intervals of 20 s from 06:00 to 10:00 on three regular workdays.

The data acquisition method adopted in this study had many advantages compared with the traditional manual measurement method [28,29]:

(*i*) Firstly, the original video data is extracted directly from the existing traffic monitoring system for the underground expressway, and the work is mainly carried out indoors, which improves the poor working environment of the traditional manual measurement method. Meanwhile, the proposed data acquisition method provides a standardized process, which makes the data acquisition process repeatable and checkable. Therefore, the data reliability is improved.

(*ii*) Secondly, the data acquisition process is relatively simple, and the number of vehicles and time intervals can be recorded on the computer. After short-term training, ordinary staff can operate the experiment, which is more efficient than the manual measurement method.

(*iii*) Finally, using the video data for indoor processing, full sample data at small time intervals (e.g., 20 s) can be obtained, but the manual measurement method is almost impossible to achieve.

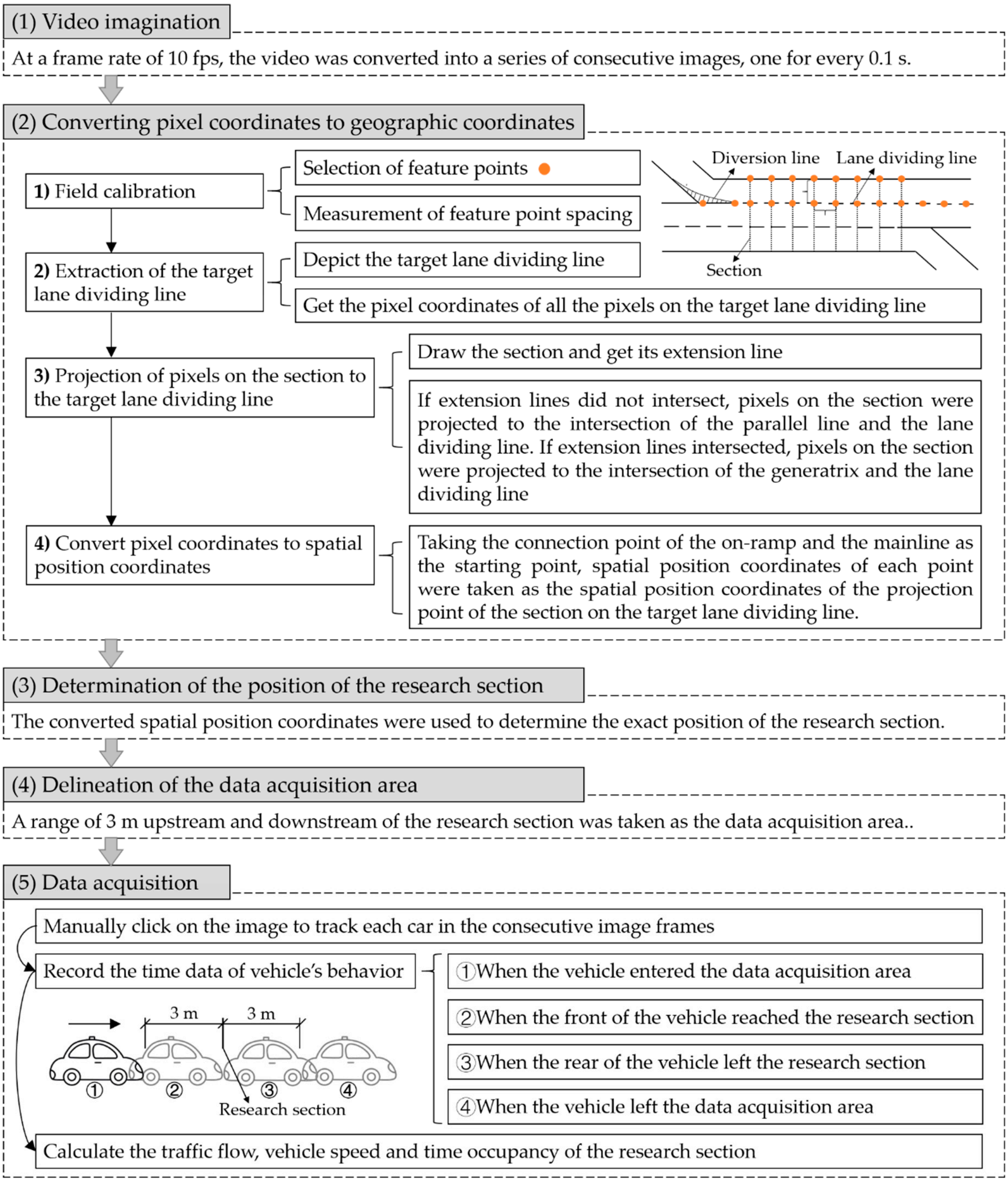

Figure 2. Flowchart for collecting data from the research section.

To analyze the difference in traffic flow characteristics between the "left-in" underground expressway and the traditional "right-in" expressway, a "right-in" expressway section with similar conditions, except for the different on-ramp layouts, was found. Thus, the section between the on-ramp of Tianyao Bridge Road and the off-ramp of Wuzhong Road, Shanghai Inner Ring Elevated Expressway was selected as the comparison section. It is equipped with a relatively complete traffic data acquisition system. Loop-coil detectors are arranged at regular intervals, and data such as traffic flow, speed, and occupancy can be collected at intervals of 20 s. The basic sketch of the selected comparison section is shown in Figure 3. The position of the red line in the figure is the detection section near coil detectors.

Similar data were collected from the research and comparison sections, including collections from similar detection positions, time intervals, data items, and so on. Additionally, the parameters of the two sections are shown in Table 1.

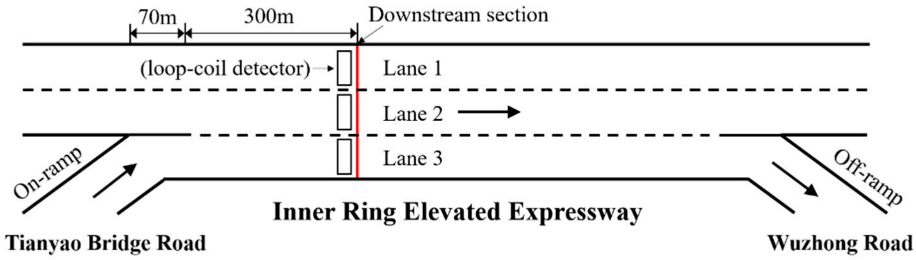

Figure 3. Sketch of "right-in" comparison section.

Table 1. Reference factors for comparison section selection.

Reference Factors	Bund Underground Expressway ("Left-In")	Inner Ring Elevated Expressway ("Right-In")
Lane width, m	3	3
On-ramp layout	Left-side of the mainline	Right-side of the mainline
Off-ramp layout	Right-side of the mainline	Right-side of the mainline
Number of on-ramp lanes	1	2 (1 lane in the merge area)
Number of lanes upstream	2	2
Number of lanes downstream	3	3
Spacing between on- and off-ramps, m	1300	1100
Design speed of the mainline, km/h	40	60
Design speed of the on-ramp, km/h	40	40
Traffic composition	Small passenger car (100%)	Small passenger car (98.8%) Medium passenger car (0.8%) Large passenger car (0.4%)

2.2. Analysis of Traffic Flow Fundamental Diagrams

The traffic flow fundamental diagram of the "left-in" underground expressway is shown in Figure 4, and the traffic flow fundamental diagram of the "right-in" elevated expressway is shown in Figure 5.

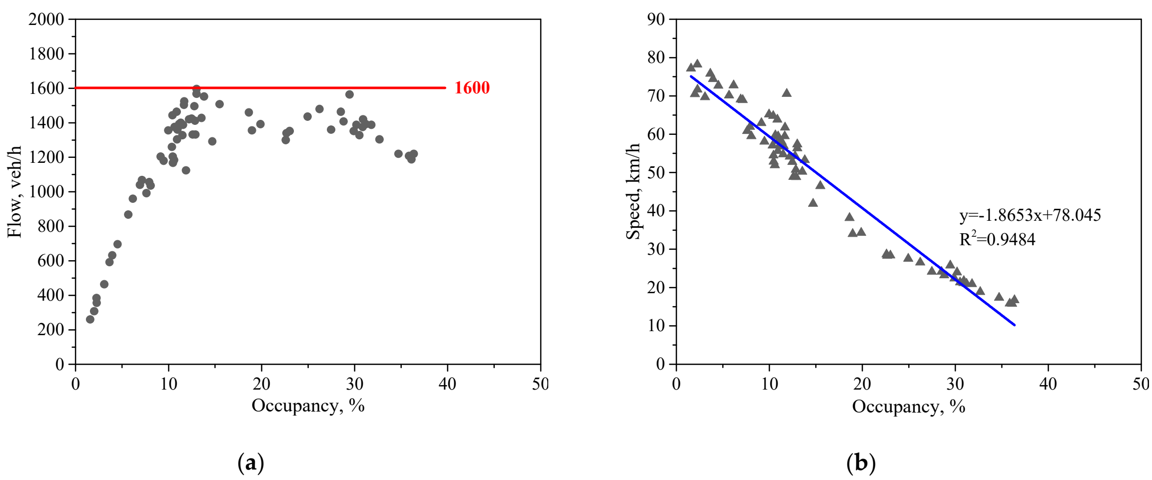

Figure 4. (**a**) Flow-occupancy scatter plot of the downstream section of the "left-in" underground expressway; (**b**) speed-occupancy scatter plot of the downstream section of the "left-in" underground expressway.

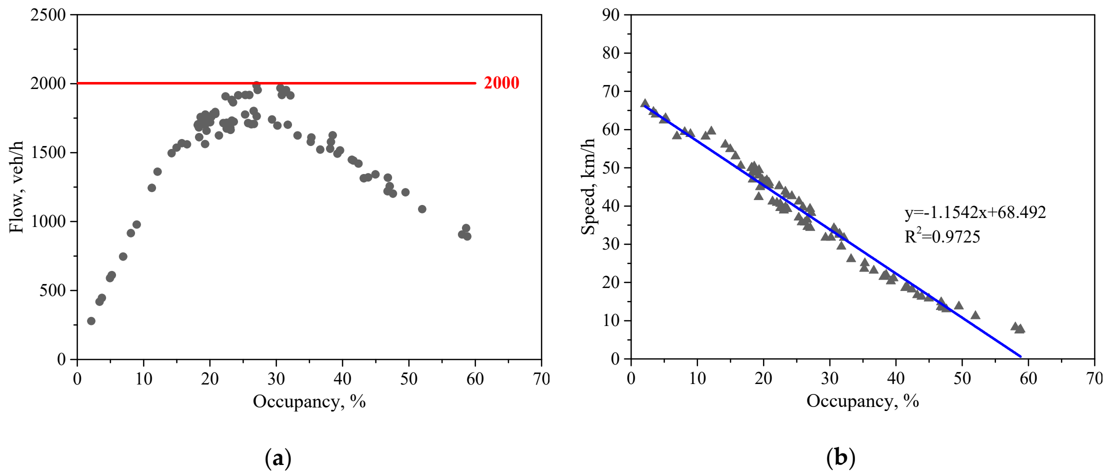

Figure 5. (**a**) Flow-occupancy scatter plot of the downstream section of the "right-in" elevated expressway; (**b**) speed-occupancy scatter plot of the downstream section of the "right-in" elevated expressway.

The comparison results of the traffic flow fundamental diagrams between the two expressway sections are shown in Table 2.

Table 2. Reference factors for comparison section selection.

Section	Fitting Formula	Fitting Degree	Free-Flow Speed, km/h	Critical Occupancy, %	Capacity, Vehicles/h
Downstream section of the "left-in" underground expressway	Y = −1.8653x+78.045	0.9484	78	22	1600
Downstream section of the "right-in" elevated expressway	Y = −1.1542x+68.492	0.9725	68	30	2000

Note: The critical occupancy is calculated from the speed-occupancy regression formula.

The analysis showed that the capacity of the "left-in" underground expressway was 20% lower than that of the "right-in" elevated expressway. The critical occupancy of the "left-in" underground expressway was 22%, while that of the "right-in" elevated expressway was 30%. The absolute value of the reduction in the critical occupancy was 8%, accounting for 27% of the critical occupancy of the "right-in" elevated expressway.

Besides that, the free-flow speed of the "left-in" underground expressway was higher than that of the "right-in" elevated expressway. Considering the lower design speed of the UES, this indicates a higher safety risk. This will be discussed in the future work.

2.3. Analysis of Speed Dispersion

The difference in speed dispersions between the "left-in" underground expressway and the "right-in" elevated expressway was analyzed. The standard deviation of speed was used to indicate speed dispersion, which has been confirmed to be correlative with the accident rate in numerous previous studies [30–32]. Therefore, this parameter was used to characterize the traffic safety features of the UES.

The speed dispersion at different occupancy levels of the two expressways is shown in Figure 6.

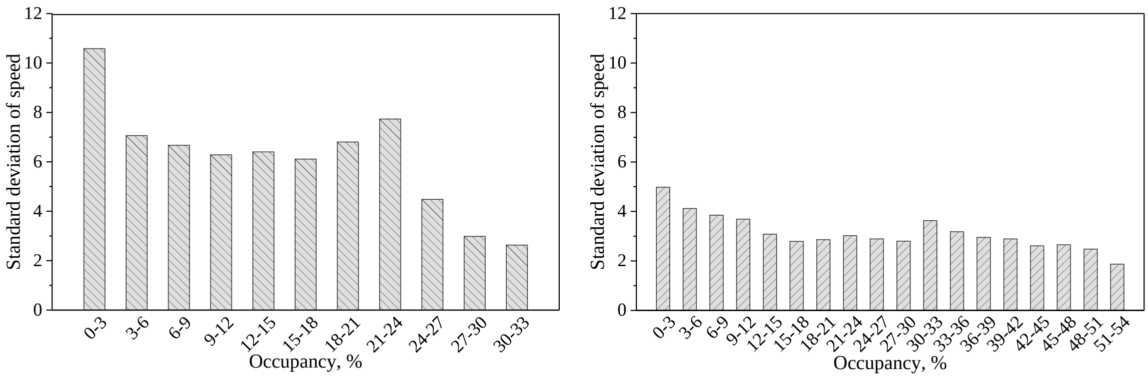

(**a**) (**b**)

Figure 6. (**a**) Standard deviation of speed in the downstream section of the "left-in" underground expressway; (**b**) standard deviation of speed in the downstream section of the "right-in" elevated expressway.

As shown in Figure 6a, when the occupancy was lower than 3%, the speed dispersion of the "left-in" underground expressway was higher, reaching 10.58. At this time, the traffic was in a free-flow state, and the mutual influence between vehicles was small, which does not bring excessive safety risks. Nevertheless, as mentioned above, due to the relatively enclosed space of the underground expressway, drivers may misjudge the driving environment and drive at a higher speed, resulting in free-flow speed that is significantly higher than the design speed and even higher than the speed of the elevated expressway used for comparison. It is recommended that a dynamic speed guidance system and strict law enforcement is adopted on the underground expressway to reduce speeding and its related risks. When the occupancy was between 3% and 18%, the speed dispersion decreased with the increase of occupancy. When the occupancy was higher than 18%, the speed dispersion showed an increasing trend, and when the occupancy was higher than 24%, the speed dispersion decreased again and remained at a lower level.

As shown in Figure 6b, the speed dispersion of the comparison section of the "right-in" elevated expressway was stable at a lower level in the occupancy range of 12% to 30%, and relatively increased after the occupancy exceeded 30%. This threshold is consistent with the critical occupancy determined in the analysis of traffic flow fundamental diagrams.

In general, when the occupancy was lower than 30%, the speed dispersion in the downstream section of the "left-in" underground expressway was significantly higher than that of the "right-in" elevated expressway. Therefore, for the underground expressway, it is very important to adopt traffic control strategies to reduce the speed dispersion.

3. A Two-Parameter On-Ramp Metering Strategy Considering Efficiency and Safety

Based on the above traffic flow characteristics of the "left-in" underground expressway, considering the traffic efficiency, safety, and efficiency of road infrastructure utilization, a novel on-ramp metering strategy for the "left-in" UES is proposed. The purpose of on-ramp metering is to increase the mainline speed, so that the mainline traffic is always operating at a smooth state without sacrificing too much efficiency in infrastructure utilization, but at the same time, reducing traffic accidents and safety risks.

3.1. Two-Parameter On-Ramp Control Model

This study used the ALINEA control model, which is one of the most representative occupancy control models. Based on the classical closed-loop feedback control strategy, the ALINEA control model maintains the occupancy downstream of the mainline in an ideal state by adjusting the on-ramp metering rate, and the occupancy is its control indicator [20,33,34]. The control model is shown in Equation (1):

$$r(k) = r(k-1) + K_R[O_c - O_{out}(k-1)] \quad (1)$$

where $r(k)$ is the on-ramp metering rate for the k-th period; $r(k-1)$ is the on-ramp metering rate for the *k-1*-th period; K_R is the adjustment parameter; O_c is the target occupancy of the mainline downstream, which is generally equal to or slightly less than the critical occupancy, which can be determined by the flow-occupancy scatter plot; and $O_{out}(k-1)$ is the measured occupancy of the mainline downstream for the *k-1*-th period.

By taking the critical occupancy as the target occupancy in most circumstances, the traditional ALINEA model allows high traffic flow that is close to capacity to pass through smoothly, which ensures high road infrastructure utilization. At the same time, as shown in Table 2 and Figure 6b, the speed dispersion of the "right-in" elevated expressway was still at a lower level under the critical occupancy, which means that lower traffic safety risks can also be achieved. In contrast, for the "left-in" UES (Table 2 and Figure 6a), the speed dispersion began to increase as critical occupancy was approached. The "left-in" UES had a higher speed dispersion, and the speed dispersion is one of the important factors affecting traffic safety [35–37].

To ensure that the traffic is operating at a smooth state and to keep the speed dispersion at a lower level, a lower target occupancy should be adopted rather than the critical occupancy. However, as the occupancy decreases, the maximum traffic flow allowed to pass through decreases, which results in a reduction in the utilization of road infrastructure. For roads in urban areas, the utilization of infrastructure should not be sacrificed too much due to the shortage of, and high demand for, road space. To balance the traffic efficiency, safety, and road infrastructure utilization in the on-ramp metering, a second control indicator, vehicle speed, was introduced into the original ALINEA model. The two-parameter on-ramp metering model for the UES is shown in Equation (2):

$$r(k) = r(k-1) + u \cdot K_R[O_t - O_{out}(k-1)] + (1-u) \cdot K_V[V_{out}(k-1)/V_c - 1] \quad (2)$$

where K_V is the speed adjustment parameter; V_c is the target speed of the mainline downstream; $V_{out}(k-1)$ is the measured speed of the mainline downstream for the *k-1*-th period; u is the weighted parameter, $0 \le u \le 1$; and the other parameters in the model are the same as those defined in Equation (1).

In Equation (2), the second item is used to ensure a smooth traffic flow and to maintain low speed dispersion. Therefore, here, it is recommended that the target occupancy O_t is a threshold value that can ensure both smooth traffic flow and low speed dispersion. Subsequently, the third item was employed to ensure smooth traffic flow and to allow for high traffic flow. To achieve this, the target speed V_c was taken as the critical speed at which traffic capacity can be obtained. The weighted parameter u was adopted to balance the control effects between these two items.

When $u = 0$, the third item of the model has the same control effect as the ALINEA model, which ensures smooth traffic and allows for high traffic flow.

When $0 < u < 1$, the second and third items control together to achieve smooth traffic, high traffic flow, and low speed dispersion. The speed dispersion control here includes two aspects: The second item controls the target occupancy to reduce the overall speed dispersion, and the third item controls the target speed to reduce the speed dispersion under an occupancy group. As the u value increases, the effect of the second item in controlling the overall speed dispersion increases, and the occupancy is close to the target occupancy. As the u value decreases, the occupancy moves closer to the critical occupancy, and the effect of the third item in controlling the speed dispersion under an occupancy group increases.

When $u = 1$, the system is completely controlled by the second item of the model. The occupancy is always maintained at less than or equal to the target occupancy to achieve a low overall speed dispersion and a smooth traffic state.

Meanwhile, considering the analysis results of the speed dispersion, the UES has a higher speed dispersion at the same occupancy level, indicating that if only the occupancy is controlled, the speed can still vary within a large range, and speeds lower than the critical speed might still occur. For example, when the occupancy is in the range of 15% to 18%, the traffic should be in a smooth state, as shown in Table 2 and Figure 4. However, speeds lower than the critical speed will still occur in an occupancy group, as shown in Figure 7. Therefore, as a byproduct, controlling speed higher than the critical speed can also decrease the speed dispersion under an occupancy group further.

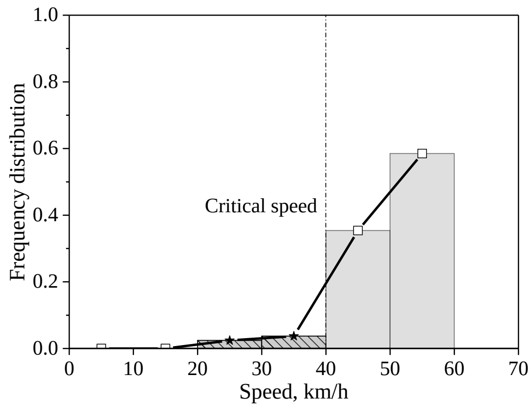

Figure 7. Speed distribution with occupancy in the range of 15% to 18%.

3.2. Target Values of Control Parameters

3.2.1. Determination of Target Occupancy

Table 2 shows that the critical occupancy is 22%, indicating a smooth traffic state. The analysis of the speed dispersion (Figure 6a) indicates that the target occupancy is 18%, ensuring low speed dispersion and high traffic efficiency. The occupancy threshold results are shown in Table 3.

Table 3. Summary of occupancy thresholds for efficiency and safety.

Optimization Objective	Efficiency	Safety
Occupancy threshold, %	22	18

3.2.2. Determination of Target Speed

Figure 4 shows that the critical speed is 40 km/h when the traffic capacity is obtained. Therefore, the speed should preferably be controlled at more than 40 km/h to ensure high traffic flow and reduce speed dispersion under an occupancy group.

In addition, other parameters in the control model were determined based on the requirements of actual control.

3.3. Mechanism of Control Model

The mechanism of the two-parameter control model was visualized under different scenarios using the measured data of the "left-in" underground expressway, as shown in Figure 8.

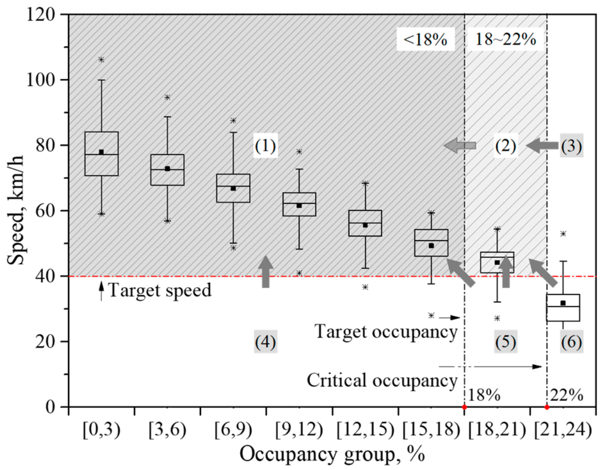

Figure 8. Mechanism of the control model under different scenarios.

In general, the control model transforms the current traffic state into the target traffic state through the following control scenarios:

(*i*) When the current traffic is at part (1) of Figure 8, it is always in a smooth state with a high traffic efficiency and a low overall speed dispersion. The control model does not play a role, and the target traffic state is the current traffic state;

(*ii*) When the current traffic is at part (2), it is in a smooth state with a high traffic efficiency and high road infrastructure utilization, but the overall speed dispersion is also high. The second item in the control model plays a major role. When the overall speed dispersion is controlled at a lower level to ensure traffic safety, the target traffic state is at part (1). From the perspective of traffic managers, when the occupancy is maintained between the target occupancy and the critical occupancy to ensure the utilization of road infrastructure, the target traffic state is still at part (2);

(*iii*) When the current traffic is in a crowded state at part (3), the second item in the control model controls the occupancy so that it is less than or equal to the critical occupancy as much as possible to ensure smooth traffic and high traffic flow, while relaxing the requirement for the overall speed dispersion, and the target traffic state is at part (2);

(*iv*) When the current traffic is at part (4), it is in a smooth state with a low traffic efficiency and low road infrastructure utilization. The third item in the model controls the speed threshold to achieve high traffic flow and reduce the speed dispersion under the occupancy group, and the target traffic state is then at part (1);

v) When the current traffic is at part (5), the second and third items control together such that the target traffic state is at part (1) or (2). Relying on the value of u to balance the control effects between the two items, the traffic is always in a smooth state;

vi) When the current traffic is in a crowded state at part (6), the target state is controlled at part (2). The second and third items control together to ensure smooth traffic and high traffic flow.

3.4. Detector Layout

Based on the requirements of the parameters in the control model, the mainline detector is arranged downstream of the mainline, about 300 m away from the entrance position. The ramp detector is arranged on the on-ramp, about 70 m from the entrance position and 2–4 m from the stop line. Additionally, the queuing detector is arranged at the end of the on-ramp.

4. Simulation Evaluation of Control Effects

4.1. Simulation Tool and Simulation Section

Based on the field investigation, VISSIM simulation software was used to establish a simulation model for the section between the left-side on-ramp of East Changzhi Road and the right-side off-ramp of Yan'an East Road, Shanghai Bund Underground Expressway. The selected simulation section was 1600 m long, including 200 m upstream of the on-ramp, 1300 m from the on-ramp to the off-ramp, and 100 m downstream of the off-ramp. Upstream of the mainline the expressway is one-way with two lanes, and downstream it is one-way with three lanes. The on-ramp is a single lane, and each lane width is 3 m. The simulation section is shown in Figure 9, and the simulation time was 120 min.

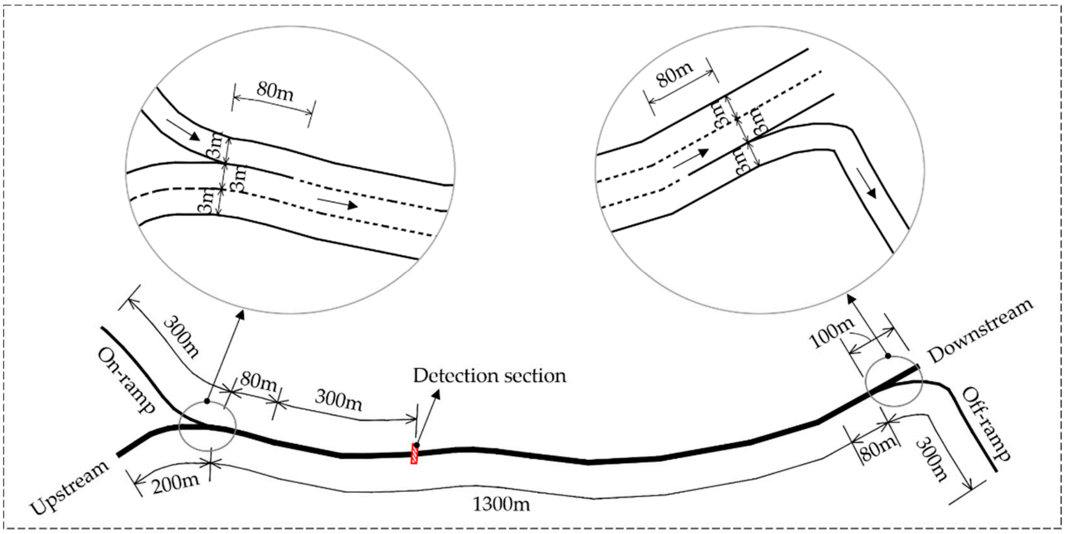

Figure 9. Model of simulation section.

4.2. Calibration of Simulation Parameters

In the process of simulation modeling, the calibration of simulation parameters has a great influence on the accuracy of the simulation.

4.2.1. Calibration Steps

The basic steps for the calibration of simulation parameters are shown in Figure 10.

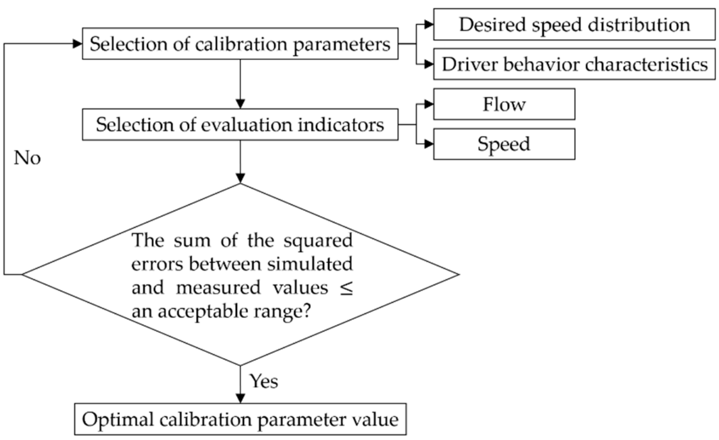

Figure 10. Flowchart for the calibration of simulation parameters.

The selected calibration parameters were the desired speed distribution and driver behavior characteristics, and the evaluation indicators were traffic flow and speed. The calibration parameters were adjusted several times until the sum of the squared errors between the simulated and measured values was within the acceptable range, and the optimal calibration parameters were obtained. These were then used as the final input parameters of the model.

4.2.2. Calibration Results

Taking the measured traffic flow data as the basic parameters, the desired speed distribution and driver behavior parameters were adjusted to improve the accuracy of the model. The calibration results of the simulation parameters were as follows:

(1) Calibration of the desired speed distribution.

The calibration of the desired speed distribution was derived from measured traffic flow data. The sections of the desired speed calibration included the upstream and downstream sections of the mainline, and the on-ramp. The specific calibration is shown in Figure 11.

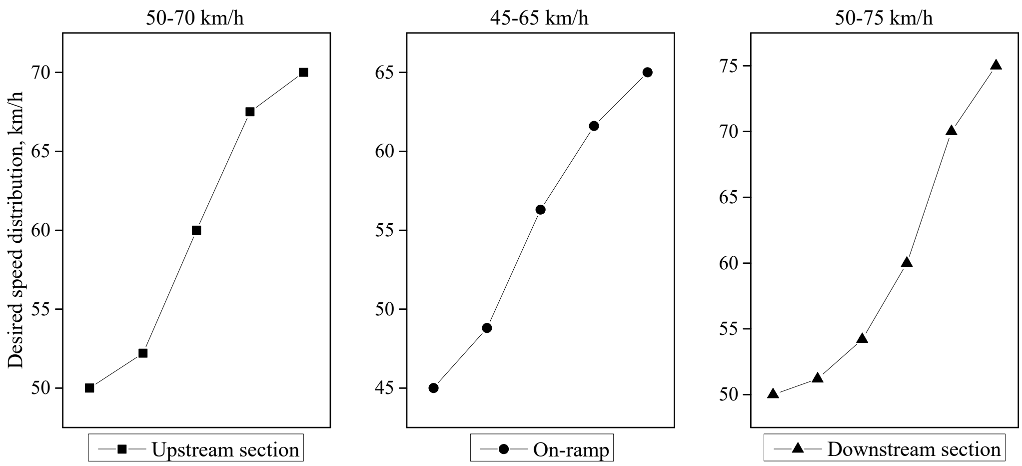

Figure 11. Desired speed distribution of the upstream section, the on-ramp, and the downstream section.

(2) Calibration of the driver behavior parameters.

The driver behavior parameters included the parameters of the car following model and the lane changing model. Using the psycho-physical Wiedemann 99 car following model for expressways, the calibrated car following model parameters were the average parking distance, the time headway, the threshold of the following state, and the vibration acceleration. Furthermore, the calibrated lane changing model parameters were the maximum deceleration, the acceptable deceleration, the safety distance reduction factor, and the maximum braking deceleration.

Selecting a certain step size, each parameter was adjusted and tested several times until the optimal calibration value was found. The final calibration results of the relevant parameters in the car following and lane changing models are shown in Table 4.

Table 4. Calibration results of key parameters in the car following and lane changing models.

	Calibration Parameter	Default Value	Calibration Value
Wiedemann 99 car following model	Parking distance, m	2.0	1.5
	Time headway, s	0.9	1.245
	Threshold of the following state, m/s	±0.35	±0.35 (default)
	Vibration acceleration, m/s^2	0.25	0.761
Lane changing vehicle	Maximum deceleration, m/s^2	–4	–4.69
	Acceptable deceleration, m/s^2	–1	–0.42
Overtaken vehicle	Maximum deceleration, m/s^2	–3	–3.62
	Acceptable deceleration, m/s^2	–0.5	–0.39
Safety distance reduction factor		0.6	0.58
Maximum braking deceleration, m/s^2		–3	–2.4

4.2.3. Evaluation of Calibration Effect

Based on the calibration results of the simulation parameters, the validity of simulation parameter calibration was verified by determining the matching effect between the flow/speed downstream of the simulation section and the measured data. The matching diagrams between the simulated flow, simulated speed, and measured data are shown in Figure 12. Moreover, the error between the simulated and the measured data was calculated and is shown in Table 5.

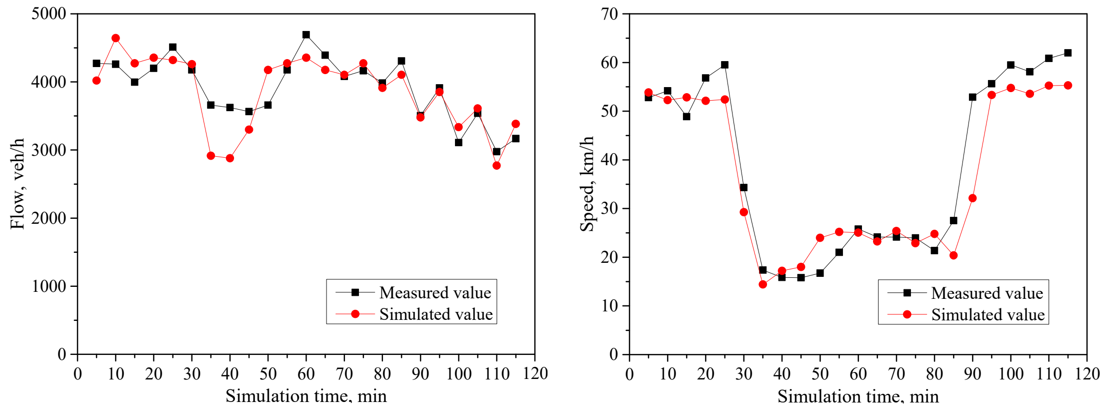

(**a**) (**b**)

Figure 12. (**a**) Matching diagram between simulated flow and measured data of the downstream section; (**b**) matching diagram between simulated speed and measured data of the downstream section.

Table 5. Error analysis between simulated data and measured data.

Time	Flow of the Downstream Section, Vehicles/h			Speed of the Downstream Section, km/h		
	Measured Value	Simulated Value	Error, %	Measured Value	Simulated Value	Error, %
7:35:00	4272	4020	6	52.79	53.85	2
7:40:00	4260	4644	9	54.19	52.26	4
7:45:00	3996	4272	7	48.89	52.83	8
7:50:00	4200	4356	4	56.82	52.14	8
7:55:00	4512	4320	4	59.52	52.40	12
8:00:00	4176	4260	2	34.32	29.27	15
8:05:00	3660	2916	20	17.35	14.41	17
8:10:00	3624	2880	21	15.84	17.20	9
8:15:00	3564	3300	7	15.79	18.00	14
8:20:00	3660	4176	14	16.73	23.98	37
8:25:00	4176	4272	2	21.01	25.21	20
8:30:00	4692	4356	7	25.79	25.05	3
8:35:00	4392	4176	5	24.15	23.24	4

Table 5. *Cont.*

Time	Flow of the Downstream Section, Vehicles/h			Speed of the Downstream Section, km/h		
	Measured Value	Simulated Value	Error, %	Measured Value	Simulated Value	Error, %
8:40:00	4080	4104	1	24.15	25.40	5
8:45:00	4164	4272	3	23.96	22.90	4
8:50:00	3984	3912	2	21.36	24.79	16
8:55:00	4308	4104	5	27.52	20.39	26
9:00:00	3504	3480	1	52.89	32.14	39
9:05:00	3912	3852	2	55.64	53.55	4
9:10:00	3108	3336	7	59.51	54.77	8
9:15:00	3540	3612	2	58.09	53.56	8
9:20:00	2976	2772	7	60.86	55.25	9
9:25:00	3168	3384	7	61.97	55.29	11
Average error, %			9			12

As shown in Table 5, the average error between the simulated and measured data was within 12%. Although there were individual errors exceeding 12%, the error was generally at a lower level. Therefore, it can be concluded that the calibration of the model parameters was sufficient and the simulated data were as close as possible to the measured data.

4.3. Control Effect Analysis

To verify the effectiveness of the proposed on-ramp metering strategy considering efficiency and safety, the control effects of the non-control, the ALINEA control strategy, and the two-parameter control strategy based on occupancy and speed were compared and analyzed. Taking into account the weight of occupancy control and speed control in the two-parameter control model, the value of u was determined to be 0.5. K_R took the classic value of 70, and K_V was taken as 50. The traffic flow, average speed, and speed fluctuation of the mainline downstream section and the queue length of the on-ramp were selected as evaluation indicators, which not only reflected the general situation of the flow and speed of the mainline to realize the speed control of the mainline, but also avoided the interference of the on-ramp queuing to the mainline.

The traffic flow generated in the VISSIM simulation was shown in Appendix A. The quantitative analysis of the simulation effects of different control strategies is shown in Table 6.

Table 6. Comparison of simulation effects.

Evaluation Indicator	Non-Control	ALINEA [1] Control	Two-Parameter Control
Traffic flow (vehicles/h)	3876	3760	3834
Effect comparison	-	–2.99%	–1.00%
Average speed (km/h)	35.50	45.83	46.45
Effect comparison	-	+22.50%	+23.50%
Speed fluctuation (km/h)	5.69	3.16	3.01
Effect comparison	-	–44.40%	–47.10%
Average number of queued vehicles on the on-ramp	-	12	7

[1] ALINEA: the acronym for 'Asservissement line' aire d'entre' e autoroutie' [15–17].

As shown in Table 6, the advantages of the two-parameter control can be explained from the following aspects.

(*i*) In terms of the traffic flow, the mainline traffic flow of the ALINEA control and the two-parameter control was slightly reduced compared to that of the non-control, but the flow reduction of the two-parameter control was lower than that of the ALINEA control. The flow of the two-parameter control was almost equal to that of the non-control.

(*ii*) In terms of the speed control, the mainline average speed of the two-parameter control increased more than that of the ALINEA control, and the speed fluctuation decreased more, so that the overall traffic conditions of the mainline significantly improved.

(*iii*) In addition, the average queue length on the on-ramp of the two-parameter control was 42% lower than that of the ALINEA control, which greatly reduced the impact on the mainline traffic.

Therefore, simultaneously taking speed and occupancy as control indicators guarantees the stability of the control strategy and has a positive effect on driving safety and efficiency.

5. Conclusions

This study explored the traffic flow characteristics of the "left-in" underground expressway based on the measured data and proposed a novel on-ramp metering strategy to improve the efficiency and safety of the UES. The main conclusions of this study are as follows:

(1) Firstly, the traffic flow fundamental diagrams between the "left-in" and "right-in" expressways were compared. The traffic capacity of the "left-in" underground expressway was shown to be 20% lower than that of the "right-in" elevated expressway, and 27% lower in terms of critical occupancy. However, the free-flow speed was higher. Meanwhile, the "left-in" underground expressway appeared to have a higher speed dispersion and; therefore, a higher accident risk.

(2) Secondly, considering the traffic efficiency, safety, and road infrastructure utilization, a novel two-parameter on-ramp metering strategy for the UES was proposed, in which speed and occupancy were used as the control indicators simultaneously. Based on the discussion of the control parameter threshold, the target occupancy value was taken as 18%, and the target speed value was 40 km/h. Based on this, the mechanism of the two-parameter control model was visualized under different scenarios using data measured from the "left-in" underground expressway.

(3) Finally, a simulation model based on measured data was established. The two-parameter control strategy was shown to be superior to the non-control and ALINEA control strategies in terms of stability and speed fluctuation control. Thus, the proposed on-ramp metering strategy for the UES was shown to be feasible and practical and can effectively ensure traffic safety and efficiency.

Therefore, this study enriches the on-ramp metering strategy for expressways in the intelligent transportation system. The on-ramp metering strategy based on the analysis of the "left-in" UES traffic characteristics can effectively improve the traffic safety and efficiency of UESs. It is suggested that future works study the reliability of the on-ramp metering strategy and extend the strategy to the left-side on-ramp of the actual underground expressway.

Author Contributions: M.S., C.X. and X.W. conceived and designed the methodology and model; X.W. analyzed the data; M.S. and C.X. interpreted the findings and wrote the paper; and L.S. and Z.C. provided revision suggestions. All the authors have read and approved the final manuscript.

Funding: This research was funded by the National Nature Science Foundation of China (No.51208379) and the Scientific Research Program Project of Shanghai Science and Technology Commission (16DZ1203602).

Acknowledgments: The authors wish to acknowledge the crucial role of our research teams (Key Laboratory of Road and Traffic Engineering of the Ministry of Education) members and all stakeholders involved in the data collection and supporting tasks. Special thanks go to Road Network Monitoring Center of Shanghai Road Administration for the data support provided to our study.

Conflicts of Interest: The authors declare no conflicts of interest.

Appendix A

The section positions of the upstream and the on-ramp where the traffic flow was generated are shown by the red lines in Figure A1. The traffic flow generated in the three simulation scenarios is shown in Table A1.

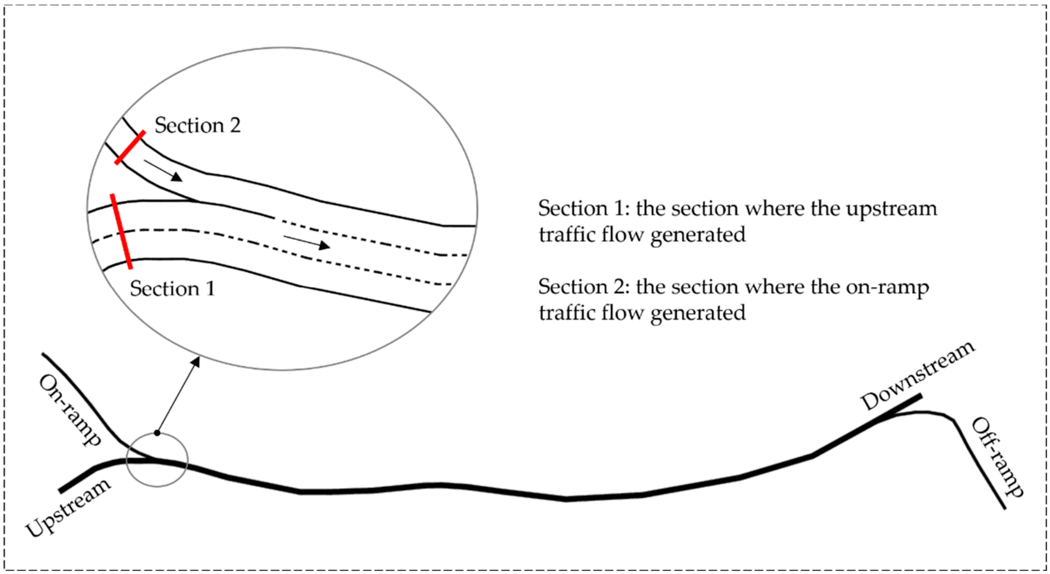

Figure A1. Section positions of the generated traffic flow.

Table A1. Traffic flow generated in the simulation.

Simulation Time, s	Upstream Traffic, Vehicles	On-Ramp Traffic, Vehicles
300	206	138
600	202	136
900	239	149
1200	215	145
1500	205	153
1800	221	146
2100	193	153
2400	185	90
2700	165	108
3000	224	105
3300	220	108
3600	213	103
3900	231	137
4200	172	131
4500	213	139
4800	195	146
5100	204	133
5400	202	125
5700	176	110
6000	206	119
6300	156	113
6600	206	103
6900	134	96
7200	179	104

References

1. Weg, G.S.V.D.; Hegyi, A.; Hoogendoorn, S.P.; Schutter, B.D. Efficient freeway MPC by parameterization of ALINEA and a speed-limited area. *IEEE Trans. Intell. Transp. Syst.* **2018**, *99*, 1–14.
2. Liu, Y. A study on merging and diverging area design for urban underground expressway. *Procedia Eng.* **2016**, *165*, 175–183. [CrossRef]
3. Yang, Y.; Li, K.; Zhu, M. Speed distribution characteristic on urban underground roads. *Sci. Technol. Eng.* **2011**, *11*, 1863–1867.

4. Luo, S. Study on the Vehicles Running Characteristics in Ramp Entrances and Exits of Urban Underground Expressway. Ph.D. Thesis, Tongji University, Shanghai, China, 2014.
5. Ma, Z.; Chien, I.J.; Dong, C.; Hu, D.; Xu, T. Exploring factors affecting injury severity of crashes in freeway tunnels. *Tunn. Undergr. Space Technol.* **2016**, *59*, 100–104. [CrossRef]
6. Sun, J.; Li, T.; Yu, M.; Zhang, H.M. Exploring the congestion pattern at long-queued tunnel sag and increasing the efficiency by control. *IEEE Trans. Intell. Transp. Syst.* **2018**, *19*, 3765–3777. [CrossRef]
7. Feng, Z.; Yang, M.; Zhang, W.; Du, Y.; Bai, H. Effect of longitudinal slope of urban underpass tunnels on drivers' heart rate and speed: A study based on a real vehicle experiment. *Tunn. Undergr. Space Technol.* **2018**, *81*, 525–533. [CrossRef]
8. Haack, A. Current safety issues in traffic tunnels. *Tunn. Undergr. Space Technol.* **2002**, *17*, 117–127. [CrossRef]
9. Calvi, A.D.; Amico, F. A study of the effects of road tunnel on driver behavior and road safety using driving simulator. *Adv. Transp. Stud.* **2013**, *30*, 59–76.
10. Liu, S.; Wang, J.; Fu, T. Effects of lane width, lane position and edge shoulder width on driving behavior in underground urban expressways: A driving simulator study. *Int. J. Environ. Res. Public Health* **2016**, *13*, 1010. [CrossRef]
11. Wei, L.; Xu, J.; Jia, X.; Zhang, X.; Li, H. Effects of safety facilities on driver distance perception in expressway tunnels. *J. Adv. Transp.* **2018**. [CrossRef]
12. Kim, G.; Lee, S.; Choi, K. Simulation-based evaluation for urban expressway ramp metering: A Madison Beltline case. *Ksce J. Civ. Eng.* **2004**, *8*, 335–342. [CrossRef]
13. Jiang, R.; Lee, J.; Chung, E. Proportional-derivative (PD) controller for heuristic rule-based motorway coordinated ramp meters. *Ksce J. Civ. Eng.* **2018**, *22*, 3644–3652. [CrossRef]
14. Wang, X.; Niu, L. Integrated variable speed limit and ramp metering control study on flow interaction between mainline and ramps. *Adv. Mech. Eng.* **2019**, *11*, 1–12. [CrossRef]
15. Papageorgiou, M.; Hadj-Salem, H.; Blosseville, J.M. ALINEA: A local feedback control law for on-ramp metering. *Transp. Res. Board* **1991**, *1320*, 58–67.
16. Papageorgiou, M.; Kotsialos, A. Freeway ramp metering: An overview. *IEEE Trans. Intell. Transp. Syst.* **2002**, *3*, 271–281. [CrossRef]
17. Demiral, C.; Celikoglu, H.B. Application of ALINEA ramp control algorithm to freeway traffic flow on approaches to Bosphorus strait crossing bridges. *Procedia Soc. Behav. Sci.* **2011**, *20*, 364–371. [CrossRef]
18. Makigami, Y.; Matsuo, T. Evaluation of outside and inside expressway ramps based on merging probability. *J. Transp. Eng.* **1991**, *117*, 57–70. [CrossRef]
19. Gao, H.; Ran, R. Local freeway ramp metering using self-adjusted fuzzy controller. *Teh. Vjesn. Tech. Gaz.* **2018**, *25*, 1174–1182.
20. Majid, H.; Lu, C.; Karim, H. An integrated approach for dynamic traffic routing and ramp metering using sliding mode control. *J. Traffic Transp. Eng. (Engl. Ed.)* **2018**, *5*, 116–128. [CrossRef]
21. Fang, J.; Tu, L. Prediction based active ramp metering control strategy with mobility and safety assessment. *Adv. Mater. Mach. Electron. II* **2018**, *1955*, 1–5.
22. Zhou, H.; Chen, H.; Zhao, J.; Hsu, P. Operational and safety performance of left-side off-ramps at freeway diverge areas. In Proceedings of the Transportation Research Board Annual Meeting, Washington, DC, USA, 10–14 January 2010.
23. Zhao, J.; Zhou, H.; Chen, H.; Hsu, P. Safety effects of left exit on freeway: A case study in Florida, USA. *Adv. Transp. Stud.* **2011**, *25*, 75–90.
24. Chen, H.; Zhou, H.; Zhao, J.; Hsu, P. Safety performance evaluation of left-side off-ramps at freeway diverge areas. *Accid. Anal. Prev.* **2011**, *43*, 605–612. [CrossRef] [PubMed]
25. Liu, Y. Research on Urban Underground Expressway Entrance Driving characteristics and Safety Design Based on Driving simulator. Master's Thesis, Tongji University, Shanghai, China, 2014.
26. Fang, S.; Jie, L.; Liu, S.; Wang, J. Vehicle operation characteristics of ramp entrance in underground road. *Syst. Simul. Technol.* **2017**, *13*, 83–89.
27. Eustace, D.; Aylo, A.; Mergia, W.Y. Crash frequency analysis of left-side merging and diverging areas on urban freeway segments—A case study of I-75 through downtown Dayton, Ohio. *Transp. Res. Part C Emerg. Technol.* **2015**, *50*, 78–85. [CrossRef]
28. Wei, J.; Zhihong, T.; Chao, C.; Bei, G. Bottleneck analysis for data acquisition in high-speed network traffic monitoring. *China Commun.* **2014**, *11*, 110–118. [CrossRef]

29. Zhou, D.; Yan, Z.; Fu, Y.; Yao, Z. A survey on network data collection. *J. Netw. Comput. Appl.* **2018**, *116*, 9–23. [CrossRef]
30. Pande, A.; Abdelaty, M. Assessment of freeway traffic parameters leading to lane-change related collisions. *Accid. Anal. Prev.* **2006**, *35*, 936–948. [CrossRef]
31. Liu, S.; Wang, J.; Zhang, L.; Fang, S. Characteristic and prediction model for operation speed model in urban underground road. *J. Tongji Univ. (Nat. Sci.)* **2015**, *43*, 1677–1683.
32. Chen, F.; Chen, S.; Ma, X. Analysis of hourly crash likelihood using unbalanced panel data mixed logit model and real-time driving environmental big data. *J. Saf. Res.* **2018**, *65*, 153–159. [CrossRef]
33. Khayatian, M. Analysis of a ramp metering application for Mitchell Freeway. In Proceedings of the Australian Institute of Traffic Planning and Management National Conference, Perth, Western Australia, 30 July–2 August 2013.
34. Abuamer, I.M.; Celikoglu, H.B. Local ramp metering strategy ALINEA: Microscopic simulation based on evaluation study on Istanbul freeways. *Transp. Res. Procedia* **2017**, *22*, 598–606. [CrossRef]
35. Pei, X.; Wong, S.C.; Sze, N.N. The roles of exposure and speed in road safety analysis. *Accid. Anal. Prev.* **2012**, *48*, 464–471. [CrossRef] [PubMed]
36. Chung, C.L.; Recker, W.W. Characteristics of speed dispersion and its relationship to fundamental traffic flow parameters. *Transp. Plan. Technol.* **2014**, *37*, 581–597. [CrossRef]
37. Liu, Y.; Li, J.; Chen, X. Traffic speed dispersion on urban expressways: The characteristics and its influence factors. *J. Transp. Syst. Eng. Inf. Technol.* **2018**, *18*, 111–120.